Topological Kondo Insulators

Maxim Dzero,[1] Kai Sun,[1] Victor Galitski,[1] and Piers Coleman[2]
[1]Joint Quantum Institute and Department of Physics, University of Maryland, College Park, Maryland 20742, USA
[2]Center for Materials Theory, Rutgers University, Piscataway, New Jersey 08854, USA
(Received 22 December 2009; published 12 March 2010)

Kondo insulators are a particularly simple type of heavy electron material, where a filled band of heavy quasiparticles gives rise to a narrow band insulator. Starting with the Anderson lattice Hamiltonian, we develop a topological classification of emergent band structures for Kondo insulators and show that these materials may host three-dimensional topological insulating phases. We propose a general and practical prescription of calculating the Z_2 topological indices for various lattice structures. Experimental implications of the topological Kondo insulating behavior are discussed.

DOI: 10.1103/PhysRevLett.104.106408 PACS numbers: 71.27.+a, 74.50.+r, 75.20.Hr

Kondo insulators are a particularly simple type of heavy fermion material, first discovered 40 years ago [1], in which highly renormalized f-electrons, hybridized with conduction electrons, form a completely filled band of quasiparticles with excitation gaps in the millivolt range [2,3]. While these materials are strongly interacting electron systems, their excitations and their ground states can be regarded as adiabatically connected to noninteracting band insulators [4].

It was recently shown that time-reversal invariant band insulators can be classified by the topological structure of their ground state wave functions [5–9]. One of the dramatic consequences of this discovery is the existence of a new class of ''topological'' band insulator in which strong spin-orbit coupling leads to a ground state that is topologically distinct from the vacuum, giving rise to gapless surface excitations.

In this Letter, we show that Kondo insulators, as adiabatic descendents of band insulators, can also be topologically classified. The strong spin-orbit coupling characteristic of these materials leads us to predict that a subset of Kondo insulators are topologically nontrivial, with anomalous surface excitations. In current models of topological insulators, the spin-orbit coupling is encoded in a spin-dependent hopping amplitudes between different unit cells. By contrast, in a topological Kondo insulator (TKI), we show that the topologically nontrivial insulating state is produced by the spin-orbit coupling associated with the hybridization between conduction and f electrons.

Below, we develop a model for topological KIs. The physics we study is motivated by the canonical Kondo insulating behavior of SmB_6 [1] and $Ce_3Bi_4Pt_3$ [10]. The realization of a particular topologically nontrivial insulating state depends on the position of renormalized f level relative to the bottom of the conduction band, Fig. 1. To analyze the topology of the bands in these materials, we use a periodic Anderson lattice model.

In a KI, the insulating state arises due to hybridization between the conduction and f electrons, provided that the chemical potential lies inside the hybridization gap separating the quasiparticle bands. The spatial symmetry of the hybridization amplitude is determined by the symmetry of the underlying crystal-field Kramers doublets of the rare-earth ion, and it is precisely this symmetry that is responsible for nontrivial topological structures in a KI. To analyze this topology, we first employ a tight-binding model on a simple cubic lattice, which is adiabatically connected to the Hamiltonian of the KI material. We show that in this case, band topology is uniquely determined by the noninteracting band structure of the system in the absence of hybridization. Second, we consider a more general KI in a lattice with a body centered cubic lattice, and show that regardless of microscopic details, there always exists a parameter range in which a KI is a strong topological insulator (STI).

We begin with the periodic Anderson Kondo lattice Hamiltonian, written in terms of the fermion operators associated with the crystal-field symmetry of the underlying lattice

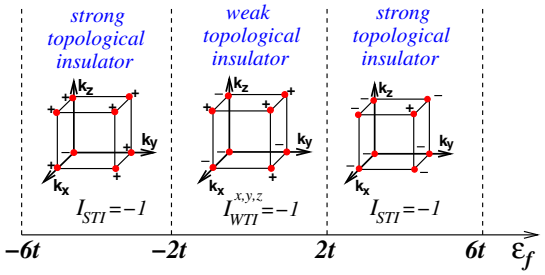

FIG. 1 (color online). Values of strong and weak topological indices and signs of δ_i (see text) at the high-symmetry points of the Brillouin zone (BZ) are shown as a function of position of the renormalized f level relative to the bottom of the conduction band. For the simple cubic tight-binding spectrum of the form $\epsilon_{\mathbf{k}} = -2t\sum_{a=x,y,z}\cos k_a$ topologically strong, weak Kondo insulating behavior as well as regular band insulator ($|\varepsilon_f| > 6t$) can be realized.

$$\hat{H} = \sum_{\mathbf{k},\alpha} \xi_{\mathbf{k}} c^{\dagger}_{\mathbf{k}\alpha} c_{\mathbf{k}\alpha} + \sum_{j\alpha} [V c^{\dagger}_{j\alpha} f_{j\alpha} + \text{H.c.}] + \sum_{j\alpha} \left[\varepsilon^{(0)}_f n_{f,j\alpha} + \frac{U_f}{2} n_{f,j\alpha} n_{f,j\bar{\alpha}} \right] \quad (1)$$

where $\xi_{\mathbf{k}}$ is the dispersion of a tight-binding band of conduction electrons. We assume that the ground state of the isolated magnetic ion is a Kramers doublet $|\Gamma\alpha\rangle$, where Γ labels a particular representation of the crystal symmetry group. For instance, in a cerium-based Kondo system, the Ce ion has a Ce^{3+} valence configuration; hence, we have one f electron in a $J = 5/2$ atomic shell. In Eq. (1) above, the operator $c^{\dagger}_{j\alpha}$ creates an electron on-site j in a Wannier state described by the quantum number $\alpha = \pm$, $\varepsilon^{(0)}_f$ is the bare energy of the f level, V is the bare hybridization, and U_f describes Hubbard repulsion between f electrons. One can relate the Wannier states at site j as follows [11]: $c_{j\alpha} = \sum_{k\sigma} [\Phi_{\Gamma\mathbf{k}}]_{\alpha\sigma} c_{\mathbf{k}\sigma} e^{i\mathbf{k}\cdot\mathbf{R}_j}$, where the form factors $[\Phi_{\Gamma\mathbf{k}}]_{\alpha\sigma}$ are two dimensional matrices

$$[\Phi_{\Gamma\mathbf{k}}]_{\alpha\sigma} = \sum_{m\in[-3,3]} \left\langle \Gamma\alpha | 3m, \frac{1}{2}\sigma \right\rangle \tilde{Y}^3_{m-\sigma}(\mathbf{k}) \quad (2)$$

where $\tilde{Y}^3_M(\mathbf{k}) = \frac{1}{Z}\sum_{\mathbf{R}\neq\mathbf{0}} Y^3_M(\hat{\mathbf{R}}) e^{i\mathbf{k}\cdot\mathbf{R}}$ is a tight-binding generalization of the spherical Harmonics that preserves the translational symmetry of the hybridization, $\Phi(\mathbf{k}) = \Phi(\mathbf{k} + \mathbf{G})$, where $\mathbf{G}$ is a reciprocal lattice vector. Here, $\mathbf{R}$ are the positions of the Z nearest neighbor sites around the magnetic ion.

The low-energy properties of the model (1) are described in terms of renormalized quasiparticles formed via strong hybridization between the c and f states and on-site repulsion U_f. In the regime where the f states are predominantly localized, we can neglect the momentum dependence of the f electron self-energy $\Sigma_f(\mathbf{k}, \omega) \simeq \Sigma_f(\omega)$ so that the effective low-energy Hamiltonian reads [12]

$$\mathcal{H}_{\text{mf}}(\mathbf{k}) = \begin{pmatrix} \xi_{\mathbf{k}}\underline{1} & \tilde{V}\Phi^{\dagger}_{\Gamma\mathbf{k}} \\ \tilde{V}\Phi_{\Gamma\mathbf{k}} & \varepsilon_f\underline{1} \end{pmatrix}, \quad (3)$$

where $\xi_{\mathbf{k}}$ is the bare spectrum of conduction electrons taken relative to the chemical potential, $\varepsilon_f = z[\varepsilon^{(0)}_f + \Sigma_f(0)]$ is the renormalized f level, $\tilde{V} = \sqrt{z}V$, $z = (1 - \partial\Sigma_f(\omega)/\partial\omega)^{-1}_{\omega=0}$, and $\underline{1}$ denotes the unit 2×2 matrix. The KI is formed if the chemical potential of the quasiparticles lies inside the hybridization gap, separating the two bands with the spectra $E_{\pm}(\mathbf{k}) = \frac{1}{2}[\xi_{\mathbf{k}} + \varepsilon_f \pm \sqrt{(\xi_{\mathbf{k}} - \varepsilon_f)^2 + 4|\tilde{V}\Delta_{\mathbf{k}}|^2}]$, with $\Delta^2_{\mathbf{k}} = \frac{1}{2}\,\text{Tr}[\Phi^{\dagger}_{\Gamma\mathbf{k}}\Phi_{\Gamma\mathbf{k}}]$.

From Eq. (2), we see that the form factors $\Phi_{\Gamma\mathbf{k}}$ are momentum-dependent unitary matrices that relate the spin quantization axes of the Bloch states and the spin-orbit coupled Wannier states. Our choice of hybridization ensures that the mean-field Hamiltonian [Eq. (3)] is a periodic function satisfying $\mathcal{H}_{\text{mf}}(\mathbf{k}) = \mathcal{H}_{\text{mf}}(\mathbf{k} + \mathbf{G})$.

Form factors are uniquely determined by the wave functions of a magnetic ion, $|\Gamma\alpha\rangle$. For a case of Ce ion, we classify the crystal-field states according to their orbital symmetry parameterized by the index $a = 1, 2, 3$ and the pseudospin quantum number ($\alpha = \pm$) [13]. Hence, we have $f^{\dagger}_{1\pm}|0\rangle = |\pm 1/2\rangle$, $f^{\dagger}_{2\pm}|0\rangle = |\pm 3/2\rangle$, and $f^{\dagger}_{3\pm}|0\rangle = |\pm 5/2\rangle$. The momentum dependence of the hybridization gap $\Delta_a(\mathbf{k})$ follows from Eq. (2). Note that for small momenta, the hybridization gap has a line of nodes along the z axis for the shapes $a = 2, 3$, but generic combinations of all three form factors contain no nodes. The key results of this Letter are most simply illustrated using the nodeless $a = 1$ Kramers doublet as the ground state of the magnetic ion.

To analyze the topology of the bands, we use the fact that topology is invariant under any adiabatic deformation of the Hamiltonian. We begin our study with a tight-binding model for a KI on a simple cubic lattice. The technical analysis is readily generalized to more complicated cases as discussed below. The most important element of the analysis is the odd parity form factor of the f electrons, $\Phi_a(\mathbf{k}) = -\Phi_a(-\mathbf{k})$. This parity property is the only essential input as far as the topological structure is concerned.

In Ref. [14], Fu and Kane demonstrate that in an insulator with time-reversal and space-inversion symmetry, the topological structure is determined by parity properties at the eight high-symmetry points, $\mathbf{k}^*_m$, in the 3D BZ which are invariant under time reversal, up to a reciprocal lattice vector: $\mathbf{k}^*_m = -\mathbf{k}^*_m + \mathbf{G}$ (see insets in Fig. 1). In our case, these symmetries require that $\mathcal{H}_{\text{mf}}(\mathbf{k}) = P\mathcal{H}_{\text{mf}}(-\mathbf{k})P^{-1}$ and $\mathcal{H}_{\text{mf}}(\mathbf{k})^T = \mathcal{T}\mathcal{H}_{\text{mf}}(-\mathbf{k})\mathcal{T}^{-1}$, where the parity matrix P and the unitary part of the time-reversal operator $\mathcal{T}$ are given by

$$P = \begin{pmatrix} \underline{1} & \\ & -\underline{1} \end{pmatrix}, \qquad \mathcal{T} = \begin{pmatrix} i\sigma_2 & \\ & i\sigma_2 \end{pmatrix}, \quad (4)$$

where σ_2 is the second Pauli matrix. For any space-inversion-odd form factor, it follows immediately that $\hat{\Phi}_a(\mathbf{k}) = 0$ at a high-symmetry point. Hence, the Hamiltonian at this high-symmetry point is simply $\mathcal{H}_{\text{mf}}(\mathbf{k}^*_m) = (\xi_{\mathbf{k}^*_m} + \varepsilon_f)I/2 + (\xi_{\mathbf{k}^*_m} - \varepsilon_f)P/2$, where I is the four-dimensional identity matrix.

The parity at a high-symmetry point is thus determined by $\delta_m = \text{sgn}(\xi_{\mathbf{k}^*_m} - \varepsilon_f)$. Four independent Z_2 topological indices [15] (one strong and three weak indices) can be constructed from δ_m: (i) The strong topological index is the product of all eight δ_m's: $I_{\text{STI}} = \prod_{m=1}^{8} \delta_m = \pm 1$; (ii) by setting $k_j = 0$ (where $j = x$, y, and z), three high-symmetry planes, $P_j = \{\mathbf{k}: k_j = 0\}$, are formed that contain four high-symmetry points each. The product of the parities at these four points defines the corresponding weak-topological index, $I^j_{\text{WTI}} = \prod_{\mathbf{k}_m\in P_j} \delta_m = \pm 1$. The existence of the three weak-topological indices in 3D is related to a Z_2 topological index for 2D systems (a weak 3D TI is similar to a stack of 2D Z_2 topological insulators).

Because there are three independent ways to stack 2D layers to form a 3D system, the number of independent weak-topological indices is also three.

A conventional band insulator has all of the four indices $I_{\mathrm{STI}} = I^x_{\mathrm{WTI}} = I^y_{\mathrm{WTI}} = I^z_{\mathrm{WTI}} = +1$, while an index $I = (-1)$ indicates a Z_2 topological state with the odd number of surface Dirac modes. For a KI with $\xi_{\mathbf{k}^*_m=0} < \varepsilon_f$ and $\xi_{\mathbf{k}^*_m\neq\mathbf{0}} > \varepsilon_f$, we find $I_{\mathrm{STI}} = -1$, and hence the Kondo insulating state is a strong topological insulator which will be robust with respect to disorder. Weak topological insulators and topologically trivial insulators can in principle be found for different band structures and different values of ε_f, Fig. 1. Although we have been specifically considering a tight-binding model with a primitive unit cell, all our conclusions apply directly to systems adiabatically connected to this model. In order to prove it explicitly and to investigate more general cases, we develop a different and more general technique similar to that proposed in Ref. [7].

We shall now study an example of a KI for the specific shape $a = 1$ and explore the parameter range in which it remains a STI. Here, the form factor is universally determined in the small-momentum limit by the f-wave symmetry of the electron orbitals and the point group symmetry of the lattice. Expression for the form factor of a Kramer's doublet Γ_1 is

$$\hat{\Phi}_{1\mathbf{k}} \propto \frac{k^3}{\sqrt{7}} \begin{bmatrix} \sqrt{3}Y^3_0(\hat{\mathbf{k}}) & -2Y^3_1(\hat{\mathbf{k}}) \\ 2Y^3_{-1}(\hat{\mathbf{k}}) & -\sqrt{3}Y^3_0(\hat{\mathbf{k}}) \end{bmatrix}, \tag{5}$$

where $\hat{\mathbf{k}} = \mathbf{k}/k$ and $Y^l_m(\hat{\mathbf{k}})$ are the spherical harmonics. At larger momenta, the form factor depends on the microscopic details of the lattice and the Kondo coupling. In general, form factor can be written as $\hat{\Phi}_{1\mathbf{k}} = \vec{m}_{\mathbf{k}} \cdot \vec{\sigma}$.

We show below that momenta where $\hat{\Phi}_{1\mathbf{k}} = 0$ are crucial in calculating the topological indices, so that our results are generic for a linear combination of all three shapes. The most obvious zero point is located in the origin as shown in Eq. (5). We now prove that this zero point is topologically protected and that its existence necessarily yields the existence of other zero points $\hat{\Phi}_{1\mathbf{k}_i} = 0$ with $\mathbf{k}_i \neq 0$ (this conclusion is similar to fermion doubling of relativistic fermions, which requires the presence of an even number of Dirac points on a compact manifold). To prove this, we draw a sphere S^2 at the origin with radius k_0 as shown in Fig. 2(b) and require $\hat{\Phi}_{1\mathbf{k}} \neq 0$ on the sphere, which enables the definition of a Chern number $C = \frac{1}{8\pi} \oint_{S^2} d\vec{S} \cdot \epsilon^{ijk} n_i (\vec{\nabla}_{\mathbf{k}} n_j) \times (\vec{\nabla}_{\mathbf{k}} n_k)$, where $n_i = m_i/\sqrt{m_x^2 + m_y^2 + m_z^2}$ and m_i is the $\hat{\sigma}_i$ component of $\hat{\Psi}_1$ as defined above. The Chern number is a topological index quantized to an integer value. For small k_0, Eq. (5) is asymptotically accurate, which gives $C = 1$. Notice that this topological index is invariant as k_0 changes adiabatically. The nonzero value of C indicates that k_0 cannot be decreased to zero smoothly, and hence a point with $\hat{\Phi}_{1\mathbf{k}} =$

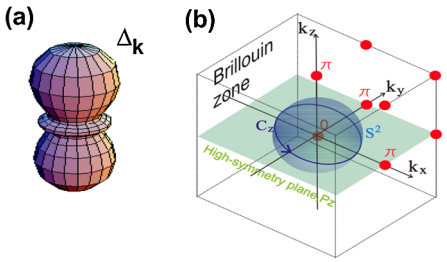

FIG. 2 (color online). (a) Surface plot of the hybridization gap $\Delta_{\mathbf{k}}$ for the form factor of shape $a = 1$, Eq. (3). The k dependence of the hybridization gap originates from the underlying orbital structure of the localized electrons, which form the magnetic moment. (b) The BZ for the BCC unit cell. Dots mark the eight high-symmetry points. The semisphere at the origin separate regions I (inside) and II (outside). The intersection of the sphere with the high-symmetry plane ($k_z = 0$) is marked by the solid line.

0 must exist inside the sphere, which ensures $\hat{\Phi}_{1\mathbf{k}=0} = 0$. Since the BZ has a periodic structure and is a compact manifold, the same argument requires zero points $\hat{\Phi}_{1\mathbf{k}_m} = 0$ outside the sphere with $|\mathbf{k}|_m > k_0$ ($m = 1, 2, \ldots$). This conclusion can be verified explicitly in the simple cubic lattice model studied above, where $\hat{\Phi}_{1\mathbf{k}} = 0$ at each of the eight high-symmetry points.

Now, we relax the assumption about the simple cubic lattice and allow for a more general structure. Because of time-reversal and space-inversion symmetries, both bands are doubly generated in a KI. Therefore, the corresponding Bloch wave functions $\Psi^1(\mathbf{k})$ and $\Psi^2(\mathbf{k})$ (which are four-component vectors) can be chosen arbitrarily up to a "local" $U(2)$ transformation in momentum space. For fermions, $\mathcal{T}^2 = -I$, and hence, we require that $\mathcal{T}\Psi^i(\mathbf{k}) = \epsilon_{ij}[\Psi^j(-\mathbf{k})]^*$ under time reversal with ϵ_{ij} being the Levi-Civita symbol. For concreteness, we focus below on the case with $\xi_{\mathbf{k}} < \varepsilon_f$ at $\mathbf{k} = 0$ and $\xi_{\mathbf{k}_i} > \varepsilon_f$ at all other zero points of $\hat{\Phi}_{1\mathbf{k}}$, which gave us a strong-topological insulator in the model with a simple cubic lattice discussed above. For such a band structure, it can be easily checked that the wave functions can *not* be defined globally in the entire BZ with the constraint $\mathcal{T}\Psi^i(\mathbf{k}) = \epsilon_{ij}[\Psi^j(-\mathbf{k})]^*$ [16]. However, the BZ can be separated into two regions (cf. Ref. [17]) I ($|\mathbf{k}| < k_0$) and II ($|\mathbf{k}| > k_0$) with k_0 being an arbitrarily small momentum such that only one zero point of $\hat{\Phi}_{1\mathbf{k}}$, $\mathbf{k} = 0$ is enclosed inside the sphere, Fig. 2(b). In each of the two regions, singularity-free Bloch wave functions can be constructed. For example, the valence band has following wave functions in region (I)

$$\begin{aligned} \Psi^1_I(\mathbf{k}) &= \mathcal{N}_-(0, \epsilon_f - E_-, -\Phi_{12}, -\Phi_{22}), \\ \Psi^2_I(\mathbf{k}) &= \mathcal{N}_-(\epsilon_f - E_-, 0, -\Phi_{11}, -\Phi_{21}), \end{aligned} \tag{6}$$

and in region (II)

$$\begin{aligned} \Psi^1_{II}(\mathbf{k}) &= \mathcal{N}_+(-\Phi^*_{21}, -\Phi^*_{22}, 0, E_+ - \epsilon_f), \\ \Psi^2_{II}(\mathbf{k}) &= \mathcal{N}_+(-\Phi^*_{11}, -\Phi^*_{12}, E_+ - \epsilon_f, 0). \end{aligned} \tag{7}$$

Here, Φ_{ij} are the (i, j) components of the form factor, $E_{\pm}(\mathbf{k})$ and $\Delta_{\mathbf{k}}$ were defined above Eq. (3), and $\mathcal{N}_{\pm} = 1/\sqrt{2\tilde{V}^2\Delta_{\mathbf{k}}^2 + (\xi_{\mathbf{k}} - \epsilon_f)(E_{\pm} - \epsilon_f)}$. These two sets of Bloch wave functions are connected by a "gauge" transformation $\Psi_I^i(\mathbf{k}) = \hat{U}_{ij}(\mathbf{k})\Psi_{II}^j(\mathbf{k})$ at the boundary, S^2, between the regions I and II, with the matrix $\hat{U}(\mathbf{k}) = -\hat{\sigma}_z\hat{\Phi}_{1-\mathbf{k}}^{\dagger}\hat{\sigma}_z/\gamma$.

The topological structure of a 3D time-reversal invariant insulator is determined by the wave functions (6) and (7), on the six high-symmetry planes $P_j = \{\mathbf{k}\colon k_j = 0\}$ and $P_j' = \{\mathbf{k}\colon k_j = \pi\}$ [6,7,14]. As shown in Fig. 2(b), the boundary between the two regions intersects with P_j and the intersections are circles, $\mathcal{C}_j$. On such a circle, the matrix $\hat{U}$ takes the form of $\hat{U}(\mathbf{k}) = \hat{\sigma}_\alpha \exp(i\varphi_0\hat{\sigma}_0 + i\varphi_{\mathbf{k}}\hat{\boldsymbol{n}}\cdot\hat{\boldsymbol{\sigma}})$, with $\hat{n}$ being a fixed 3D unit vector, corresponding to a specific "gauge." As a result, a winding number can be defined on $\mathcal{C}$ as $w_j = \oint_{\mathcal{C}_j}\frac{d\mathbf{k}}{2\pi}\cdot\nabla_{\mathbf{k}}\varphi_{\mathbf{k}}$. However, it is defined modulo 2 only because a gauge transformation can change $\varphi_{\mathbf{k}} \to \varphi_{\mathbf{k}} + 2m\phi$ and hence change w_j by an even number $2m$, where ϕ is the azimuth angle of $\mathbf{k}$ in a high-symmetry plane {note that a transformation $\varphi_{\mathbf{k}} \to \varphi_{\mathbf{k}} + (2m+1)\phi$ would violate the symmetry constraint $\mathcal{T}\Psi^i(\mathbf{k}) = \epsilon_{ij}[\Psi^j(-\mathbf{k})]^*$}. For P_j', the corresponding winding numbers w_j' are zero for the case we studied here because they do not intersect with the boundary. The topological indices can be computed from these winding numbers as follows:

$$I_{\mathrm{STI}} = (-1)^{w_j + w_j'} \quad \text{and} \quad I_{\mathrm{WTI}}^j = (-1)^{w_j}, \tag{8}$$

where I_{STI} is equivalently defined for $j = x$, y, or z. For the types of KI band structures considered here, the topological indices can be universally determined by choosing a small enough k_0 and using the asymptotic form factor of Eq. (5). As a result, we find that the generic Kondo system is a STI in full agreement with arguments above based on adiabatic deformation of the Hamiltonian onto a simple cubic lattice.

Let us briefly discuss the implications of our results for existing Kondo insulators. From our theory, we expect that materials in which f electrons are close to integral valence are likely to be weak-topological Kondo insulators and thus are unstable with respect to disorder. An interesting example is SmB_6 for which recent LSDA + U band structure calculations [18] show the position of the f level equals approximately one sixth of the bandwidth consistent with the core-level spectroscopy measurements of the f level occupation $n_f \sim 0.7$ [19], placing the quasiparticle f level of SmB_6 close to the border separating STI and WTI phases. Another promising candidate for the manifestation of topologically nontrivial insulating state is CeNiSn. Recent transport data in CeNiSn [20] show suppression of semiconducting behavior in resistivity with increase in sample's quality, although there is an evidence for the gap formation at $T \simeq 10$ K. Given that the f electrons in these systems are predominantly localized, it is tempting to speculate that the CeNiSn is a weak-topological Kondo insulator ascribing the semimetallic transport properties to metallic surface states. These are issues that we hope can be resolved in the near future through more accurate modelling and the use of high precision ARPES and STEM spectroscopy.

To summarize, we have developed a theory of topological 3D Kondo insulators. Within our model, topologically nontrivial insulating states are realized over a wide parameter range. In particular, we have shown that a strong topological insulating state occurs when the position of the renormalized f level is near the top, or the bottom of the conduction band. This suggests the most likely candidates for this kind of behavior are heavy fermion materials which are more mixed valent or have narrow conduction bands.

The results contained in this Letter were supported by the Defense Advanced Research Projects Agency (M. D. and V. G.), JQI-NSF-PFC (K. S.), NSF-CAREER (V. G.), and DOE Grant No. DE-FG02-99ER45790 (P. C.). We would like to thank Joel Moore and David Vanderbilt for discussions related to this project.

[1] A. Menth, E. Buehler, and T. H. Geballe, Phys. Rev. Lett. **22**, 295 (1969).
[2] For a review, see e.g. P. Coleman, *Handbook of Magnetism and Advanced Magnetic Materials* (Wiley, New York, 2007), Vol. 1, p. 95–148.
[3] G. Aeppli and Z. Fisk, Comments Condens. Matter Phys. **16**, 155 (1992); H. Tsunetsugu, M. Sigrist, and K. Ueda, Rev. Mod. Phys. **69**, 809 (1997); P. Riseborough, Adv. Phys. **49**, 257 (2000).
[4] R. Martin and J. Allen, J. Appl. Phys. **50**, 7561 (1979).
[5] L. Fu, C. L. Kane, and E. J. Mele, Phys. Rev. Lett. **98**, 106803 (2007).
[6] J. E. Moore and L. Balents, Phys. Rev. B **75**, 121306(R) (2007).
[7] Rahul Roy, Phys. Rev. B **79**, 195321 (2009).
[8] X. L. Qi, T. L. Hughes, and S. C. Zhang, Phys. Rev. B **78**, 195424 (2008).
[9] G. E. Volovik, Pis'ma Zh. Eksp. Teor. Fiz. **91**, 61 (2010).
[10] M. F. Hundley *et al.*, Phys. Rev. B **42**, 6842 (1990).
[11] B. Coqblin and J. R. Schriefer, Phys. Rev. **185**, 847 (1969).
[12] H. Ikeda and K. Miyake, J. Phys. Soc. Jpn. **65**, 1769 (1996).
[13] Juana Moreno and P. Coleman, Phys. Rev. Lett. **84**, 342 (2000).
[14] Liang Fu and C. L. Kane, Phys. Rev. B **76**, 045302 (2007).
[15] A. Kitaev, arXiv:0901.2686v2.
[16] Liang Fu and C. L. Kane, Phys. Rev. B **74**, 195312 (2006).
[17] M. Cheng, K. Sun, V. Galitski, and S. Das Sarma, Phys. Rev. B **81**, 024504 (2010).
[18] V. N. Antonov, B. Harmon, and A. N. Yaresko, Phys. Rev. B **66**, 165209 (2002).
[19] J. N. Chazalviel *et al.*, Phys. Rev. B **14**, 4586 (1976).
[20] T. Terashima *et al.*, Phys. Rev. B **66**, 075127 (2002).